International Journal of Mathematics and
Computer Science, **19**(2024), no. 3, 771–789

A Numerical Approximation of Conformable Maxwell-Schrodinger Equations

Kan Thotakul[1], **Anirut Luadsong**[1,2]

[1]Department of Mathematics
Faculty of Science
King Mongkut's University of Technology Thonburi (KMUTT)
Bangkok 10140, Thailand

[2]Ratchaburi Learning Park
King Mongkut's University of Technology Thonburi (KMUTT)
Ratchaburi 70150, Thailand

email: kan.tho@mail.kmutt.ac.th, anirut.lua@kmutt.ac.th

(Received December 20, 2023, Accepted January 24, 2024,
Published February 12, 2024)

Abstract

A fractional Finite-Difference Time-Domain (FDTD) method for solving conformable Maxwell–Schrodinger equations is adapted from the classical FDTD method and fractional discretization. Maxwell-Schrodinger equations model the interaction between external electromagnetic fields and quantum particles in inhomogeneous materials and the population inversion can be computed from their numerical solution. Here, parameter adjustments are shown via numerical experiments which are divided into two cases. In the first case, the fractional order parameter is set to one. Adjusting the time-step parameter to less than one increases the frequency of the population inversion, whereas adjusting the step-size parameter to less than one decreases the frequency of the population inversion. In the second case, the fractional order parameter is set to less than one. Increasing the frequency of the population inversion significantly, alongside a loss of smoothness and amplitude.

Key words and phrases: Conformable Maxwell–Schrodinger Equations, Fractional Discretization, Fractional Finite-Difference Time-Domain, Population Inversion.
AMS (MOS) Subject Classifications: 35R11, 65N06, 70H05, 81V10.
ISSN 1814-0432, 2024, http://ijmcs.future-in-tech.net

1 Introduction

Electromagnetic (EM) theory is a branch of physics that studies the EM force carried by electric and magnetic fields. EM theory can be described by the set of equations proposed by Maxwell in 1864 [1, 2]. Subsequently, Maxwell's equations evolved from the classical model to a fractional model, based on fractional calculus, and associated with non-integer order derivatives and integrals [3, 4, 5]. The fractional Maxwell equations were developed from the Caputo derivative and applied to media demonstrating fractional nonlocal properties [6]. Later, the Maxwell equations were developed into the general conformable Maxwell equations based on the general conformable fractional derivative (GCFD) [7, 8] for inhomogeneous media or materials with local properties [8].
In this paper, we use the Chen et al. model [9] and the general conformable Maxwell equations to develop the conformable Maxwell-Schrodinger equations. Our model describes the quantum particle transition between different energies as particles absorb and emit electromagnetic waves in inhomogeneous materials. The solution to this system is essential to the physics of electromagnetic sources [10, 11] and cavity quantum electrodynamics [12, 13].

Since the conformable Schrodinger-Maxwell equations are derived from Maxwell's equations and Schrodinger by the Hamilton equation, it is difficult to find the analytical solution. Instead, a solution can be obtained by the Finite-Difference Time-Domain (FDTD) method, which is a popular computational approach [14]. In 1966, Yee [15] proposed the FDTD method showing that derivatives with respect to space and time can be approximated by finite-difference methodology. The FDTD method is effective and simple to apply to a variety of problems. A fractional discretization technique has recently been proposed by Atangana [16]. This concept can be used to approximate differential operators with integer and non-integer orders. Here, we combine the classical FDTD method with fractional discretization to create a fractional FDTD method.

In Section 2, we present the details of Hamilton's equations for EM and quantum systems that lead to the conformable Schrodinger-Maxwell equations. The multi-scale issue is caused by the distinct wavelength mismatch between the EM wave and the particle wave, so it can be mitigated using the reduced eigenmode expansion technique. In Section 3, the conformable Schrodinger-Maxwell equations are discretized using our fractional FDTD

method. In Section 4, the population inversion is obtained from the numerical solution and the parameters are adjusted for comparison of the classical model with the conformable derivative model.

2 Problem Formulation

2.1 The General Conformable Maxwell Equations

We begin with the curl of the general conformable Maxwell's equations [8]

$$Curl^{\alpha,\varphi}\mathbf{D}(\mathbf{r},t) = -\epsilon_0 \frac{\partial \mathbf{B}(\mathbf{r},t)}{\partial t}, \tag{2.1}$$

$$Curl^{\alpha,\varphi}\mathbf{H}(\mathbf{r},t) = \frac{\partial \mathbf{D}(\mathbf{r},t)}{\partial t} + \mathbf{J}(\mathbf{r},t), \tag{2.2}$$

where $\mathbf{D}$ denotes electric flux density, $\mathbf{B}$, and $\mathbf{H}$ denote magnetic flux density and magnetic fields, respectively, ϵ_0 is the permittivity of free space, and $\mathbf{J}$ is the current density of external sources. $\varphi(\mathbf{r},\alpha)$ is the fractional conformable function and $\alpha \in (0,1]$. Let $\varphi(\mathbf{r},\alpha) = \varphi(x,\alpha)$. The general conformable Maxwell's equations can be defined by

$$\varphi(x,\alpha) Curl\mathbf{D}(\mathbf{r},t) = -\epsilon_0 \frac{\partial \mathbf{B}(\mathbf{r},t)}{\partial t}, \tag{2.3}$$

$$\varphi(x,\alpha) Curl\mathbf{H}(\mathbf{r},t) = \frac{\partial \mathbf{D}(\mathbf{r},t)}{\partial t} + \mathbf{J}(\mathbf{r},t). \tag{2.4}$$

2.2 The Schrodinger Equation under an EM Wave

The Schrodinger equation in an EM wave is given as

$$\left\{ \frac{1}{2m}\left[\hat{\mathbf{p}} - q\mathbf{A}(\mathbf{r},t)\right]^2 + q\phi(\mathbf{r},t) + V(\mathbf{r}) \right\} \psi(\mathbf{r},t) = i\hbar \frac{\partial \psi(\mathbf{r},t)}{\partial t}, \tag{2.5}$$

where m is the mass of the particle, $V(\mathbf{r})$ is the electrostatic potential energy, $\hbar$ is the reduced Planck's constant, q is the electric charge of the particle, $\mathbf{A}(\mathbf{r},t)$, and $\phi(\mathbf{r},t)$ are the magnetic and electric potentials, respectively, associated with the EM field, and $\hat{\mathbf{p}}$ is the momentum operator defined by

$$\hat{\mathbf{p}} = -i\hbar\nabla. \tag{2.6}$$

The fields themselves are given by

$$\mathbf{B} = \nabla \times \mathbf{A}. \tag{2.7}$$

For the Coulomb gauge, the electric potential $\phi = 0$ and the magnetic potential $\mathbf{A}$ satisfies the transversality condition $\nabla \cdot \mathbf{A} = 0$ [17]. Thus, Eq.(2.5) becomes

$$\left\{ \frac{1}{2m} \left[\hat{\mathbf{p}} - q\mathbf{A}(\mathbf{r}, t) \right]^2 + V(\mathbf{r}) \right\} \psi(\mathbf{r}, t) = i\hbar \frac{\partial \psi(\mathbf{r}, t)}{\partial t}. \tag{2.8}$$

2.3 The Hamilton Equations of the EM and QM Parts

We defined an auxiliary variable $\mathbf{Y}$,

$$\mathbf{Y} = -\mathbf{D}. \tag{2.9}$$

Following that, the total Hamiltonian of the conformable Maxwell–Schrodinger system can be expressed as

$$H(\mathbf{A}, \mathbf{Y}, \psi, \psi^*) = H^{em}(\mathbf{A}, \mathbf{Y}) + H^q(\psi, \psi^*, \mathbf{A}), \tag{2.10}$$

where

$$H^{em}(\mathbf{A}, \mathbf{Y}) = \int_\Omega \left(\frac{\varphi(x, \alpha)}{2\epsilon_0} |\mathbf{Y}|^2 + \frac{\varphi(x, \alpha)}{2\mu_0} |\nabla \times \mathbf{A}|^2 \right) dr, \tag{2.11}$$

$$H^q(\psi, \psi^*, \mathbf{A}) = \int_\Omega \left(\psi^* \frac{(\hat{\mathbf{p}} - q\mathbf{A})^2}{2m} \psi + \psi^* V \psi \right) dr. \tag{2.12}$$

In Eq.(2.10), H^{em} consists of the electric and magnetic energy stored in the EM field, and H^q consists of the kinetic and potential energy of the quantum system. The Hamilton equations for the EM and QM parts are as follows

$$\frac{\partial \mathbf{A}}{\partial t} = \frac{\partial H}{\partial \mathbf{Y}} = \frac{\varphi(x, \alpha)}{\epsilon_0} \mathbf{Y}, \tag{2.13}$$

$$\frac{\partial \mathbf{Y}}{\partial t} = -\frac{\partial H}{\partial \mathbf{A}} = -\frac{\varphi(x, \alpha)}{\mu_0} (\nabla \times \nabla \times \mathbf{A}) + \mathbf{J}, \tag{2.14}$$

$$\frac{\partial \psi}{\partial t} = \frac{1}{i\hbar} \frac{\partial H}{\partial \psi^*} = \frac{1}{i\hbar} \left[\frac{(\hat{\mathbf{p}} - q\mathbf{A})^2}{2m} + V \right] \psi, \tag{2.15}$$

$$\frac{\partial \psi^*}{\partial t} = -\frac{1}{i\hbar}\frac{\partial H}{\partial \psi} = -\frac{1}{i\hbar}\left[\frac{\left(\hat{\mathbf{p}} - q\mathbf{A}\right)^2}{2m} + V\right]\psi^*, \tag{2.16}$$

where $\mathbf{J}$ can be expressed as

$$\mathbf{J} = \frac{q}{2m}\left[\psi^*\left(\hat{\mathbf{p}} - q\mathbf{A}\right)\psi + \psi\left(-\hat{\mathbf{p}} - q\mathbf{A}\right)\psi^*\right]. \tag{2.17}$$

Eqs.(2.13)-(2.16) are known as the conformable Maxwell-Schrodinger equations. Using the vector calculus identity

$$\nabla \times \nabla \times \mathbf{A} = \nabla(\nabla \cdot \mathbf{A}) - \nabla^2\mathbf{A}, \tag{2.18}$$

and the Coulomb gauge condition, Eq.(2.14) gives the following expression

$$\frac{\partial \mathbf{Y}}{\partial t} = \frac{\varphi(x,\alpha)}{\mu_0}\left(\nabla^2\mathbf{A}\right) + \mathbf{J}, \tag{2.19}$$

where μ_0 is the permeability of a vacuum.

2.4 The Reduced Eigenmode Expansion Technique

The fractional FDTD method has an efficiency problem caused by the wavelength of the EM wave being larger than that of the particle wave, resulting in a wavelength mismatch. This issue can be mitigated by using the reduced eigenmode expansion technique. The time-dependent wave function can be expressed as follows

$$\psi(\mathbf{r},t) = a(t)exp\left(-i\omega_g t\right)\varphi_g(\mathbf{r}) + b(t)exp\left(-i\omega_e t\right)\varphi_e(\mathbf{r}), \tag{2.20}$$

where $a(t)$ and $b(t)$ are the unknown expansion coefficients. The terms $exp\left(-i\omega_g t\right)$ and $exp\left(-i\omega_e t\right)$ describe the time evolution of the eigenstates $\varphi_g(\mathbf{r})$ and $\varphi_e(\mathbf{r})$, respectively. ω_g, and ω_e are the angular frequencies of the oscillator, which are respectively for the ground and excited states. The squared magnitudes represent the probabilities of occupying the corresponding quantum states, which satisfy the probability conserving relationship shown below

$$|a(t)|^2 + |b(t)|^2 = 1. \tag{2.21}$$

By applying the Galerkin test, we have

$$\left\langle \varphi_g \middle| \frac{\partial \psi}{\partial t} \right\rangle = \left\langle \varphi_g \middle| \frac{1}{i\hbar}\frac{\partial H}{\partial \psi^*} \right\rangle, \tag{2.22}$$

$$\left\langle \varphi_e \middle| \frac{\partial \psi}{\partial t} \right\rangle = \left\langle \varphi_e \middle| \frac{1}{i\hbar} \frac{\partial H}{\partial \psi^*} \right\rangle, \tag{2.23}$$

where the inner product is defined as

$$\langle \varphi_i(\mathbf{r}) | \varphi_j(\mathbf{r}) \rangle = \int_\Omega d\mathbf{r} \varphi_i^*(\mathbf{r}) \cdot \varphi_j(\mathbf{r}). \tag{2.24}$$

According to the orthonormality of the eigenmodes,

$$\langle \varphi_i(\mathbf{r}) | \varphi_j(\mathbf{r}) \rangle = \begin{cases} 1, i = j \\ 0, i \neq j \end{cases}, \tag{2.25}$$

and the selection rule governing the parity of eigenmodes,

$$\langle \varphi_i(\mathbf{r}) | \hat{\mathbf{p}} | \varphi_i(\mathbf{r}) \rangle = 0. \tag{2.26}$$

We can get the following two ordinary differential equations

$$i\hbar \frac{da(t)}{dt} = -\frac{q\mathbf{A}}{m} \langle \varphi_g | \hat{\mathbf{p}} | \varphi_e \rangle \, b(t) e^{-i\omega_0 t} + \frac{q^2 \mathbf{A}^2}{2m} a(t), \tag{2.27}$$

$$i\hbar \frac{db(t)}{dt} = -\frac{q\mathbf{A}}{m} \langle \varphi_e | \hat{\mathbf{p}} | \varphi_g \rangle \, a(t) e^{i\omega_0 t} + \frac{q^2 \mathbf{A}^2}{2m} b(t), \tag{2.28}$$

where $\omega_0 = \omega_e - \omega_g$ denotes the transition frequency.
Finally, Eqs.(2.13),(2.19),(2.27), and (2.28) constitute a complete system that can be solved by using the fractional FDTD method. Once the expansion coefficients in Eq.(2.20) are numerically obtained, the population inversion can be defined as

$$W(t) = |b(t)|^2 - |a(t)|^2 . \tag{2.29}$$

3 Fractional Discretization

The fractional FDTD method that we describe here is adapted from the classical FDTD model and fractional discretization [16]. We focus $\mathbf{A}$ and $\mathbf{Y}$ in the y-direction denoted by A_y and Y_y, respectively. A_y and Y_y are placed at the midpoints of edges oriented in the y-direction. Thus, A_y and Y_y are on the half-grid in y. We discrete Eqs.(2.13),(2.19),(2.27), and (2.28) and

rearrange yields the following results

$$Y_y|_{i,j+\frac{1}{2},k}^{n+\frac{\gamma}{2}} = Y_y|_{i,j+\frac{1}{2},k}^{n-\frac{\gamma}{2}} + \frac{(\gamma\Delta t)\varphi(x_i,\alpha)}{(\beta\Delta x)^2\mu_0}\left[A_y|_{i+\beta,j+\frac{1}{2},k}^{n} - 2A_y|_{i,j+\frac{1}{2},k}^{n} + A_y|_{i-\beta,j+\frac{1}{2},k}^{n}\right] + \frac{(\gamma\Delta t)\varphi(x_i,\alpha)}{(\beta\Delta z)^2\mu_0}\left[A_y|_{i,j+\frac{1}{2},k+\beta}^{n} - 2A_y|_{i,j+\frac{1}{2},k}^{n} + A_y|_{i,j+\frac{1}{2},k-\beta}^{n}\right] + J_y|_{i,j+\frac{1}{2},k}^{n} \tag{3.30}$$

$$A_y|_{i,j+\frac{1}{2},k}^{n+\gamma} = A_y|_{i,j+\frac{1}{2},k}^{n} + \frac{(\gamma\Delta t)\varphi(x_i,\alpha)}{\epsilon_0}Y_y|_{i,j+\frac{1}{2},k}^{n+\gamma}, \tag{3.31}$$

$$a|^{n+\gamma} = -\frac{q(\gamma\Delta t)}{i\hbar m}A_y|^n \left\langle\varphi_g|\hat{\mathbf{p}}|\varphi_e\right\rangle b|^n e^{-i\omega_0 t_n} + \left[\frac{q^2(\gamma\Delta t)}{2i\hbar m}A_y^2|^n + 1\right]a|^n, \tag{3.32}$$

$$b|^{n+\gamma} = -\frac{q(\gamma\Delta t)}{i\hbar m}A_y|^n \left\langle\varphi_e|\hat{\mathbf{p}}|\varphi_g\right\rangle a|^n e^{i\omega_0 t_n} + \left[\frac{q^2(\gamma\Delta t)}{2i\hbar m}A_y^2|^n + 1\right]b|^n. \tag{3.33}$$

where $0 < \beta, \gamma \leq 1$. A_y and Y_y are defined on the same collocated grids. The values $\left\langle\varphi_g|\hat{\mathbf{p}}|\varphi_e\right\rangle, \left\langle\varphi_e|\hat{\mathbf{p}}|\varphi_g\right\rangle$ are defined by

$$\left\langle\varphi_g|\hat{\mathbf{p}}|\varphi_e\right\rangle = -i\sqrt{\frac{\hbar m\omega}{2}}, \tag{3.34}$$

$$\left\langle\varphi_e|\hat{\mathbf{p}}|\varphi_g\right\rangle = i\sqrt{\frac{\hbar m\omega}{2}}. \tag{3.35}$$

The initial values of the expansion coefficients a, and b, the vector potential A_y and the auxiliary variable Y_y need to be predefined.

4 Numerical Experiments

Several results are presented in this section to shift in numerical solutions when the parameters α, β, and γ are changed. If the dimension of a nanocavity is set to $L_x = L_y = L_z = 40$ nm with a spatial grid of 1 nm, then the following initial condition is created [9]

$$Y_y|_{t=0} = -\epsilon_0 A_0 sin\left(\frac{\pi}{L_x}x\right) sin\left(\frac{\pi}{L_z}z\right) cos(\omega t)|_{t=0}, \tag{4.36}$$

where

$$\omega = c\sqrt{\left(\frac{\pi}{L_x}\right)^2 + \left(\frac{\pi}{L_z}\right)^2}. \tag{4.37}$$

c is the speed of light. Here we set $A_0 = 10^{10}$ V/m and used a time increment, 6.75×10^{-19} s. A_y vanishes at the boundary of a closed resonant cavity, thus guaranteeing a unique solution. As the particle resides at the center of this cavity and is initially prepared in a superposition state with $a = 1/\sqrt{2}$ and $b = i/\sqrt{2}$, the resonant working frequency of the cavity ω is equal to the transition frequency of the particle ω_0.

4.1 The Population Inversion $W(t)$ from The Conformable Maxwell–Schrodinger Equations by Setting $\alpha = 1$

Here, we set $\alpha = 1$. The population inversion $W(t)$ obtained by setting $\beta = 1$ and $\gamma = 1$ is shown in Figure 1. The particle oscillates periodically between its ground and excited states. When the particle is illuminated by EM waves in the cavity, it cyclically absorbs photons and re-emits them.

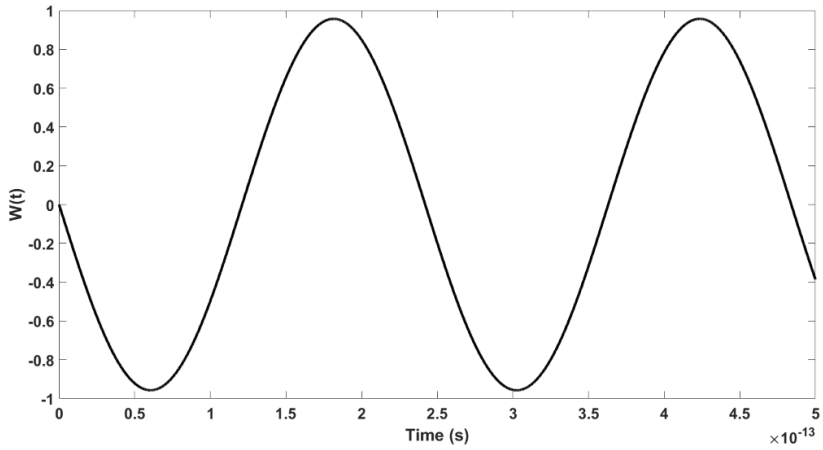

Figure 1: The population inversion $W(t)$ by setting $\alpha = 1$, $\beta = 1$, and $\gamma = 1$

Figure 2 shows the population inversion $W(t)$ by setting $\beta = 1$ and $\gamma = 0.8$. We can see that when γ is less than 1, the frequency of $W(t)$ is slightly increased when compared with $W(t)$ in Figure 1. The same effect is observed in Figures 3 and 4 by setting $\beta = 1$ and adjusting γ to 0.625 and 0.4, respectively.

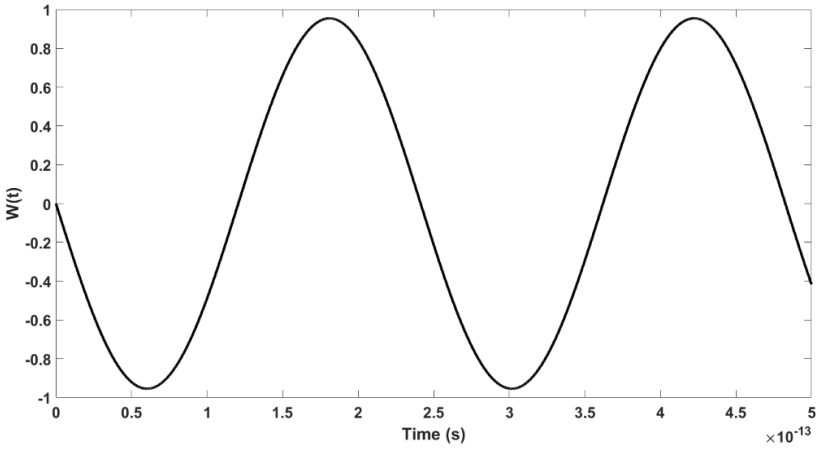

Figure 2: The population inversion $W(t)$ by setting $\alpha = 1$, $\beta = 1$, and $\gamma = 0.8$

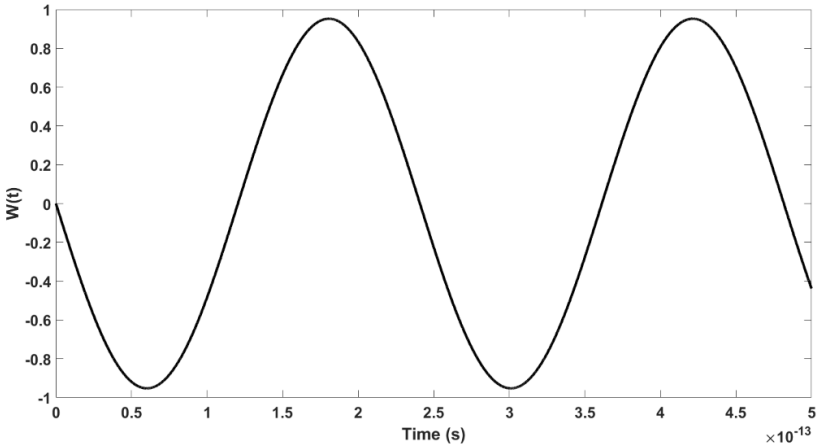

Figure 3: The population inversion $W(t)$ by setting $\alpha = 1$, $\beta = 1$, and $\gamma = 0.625$

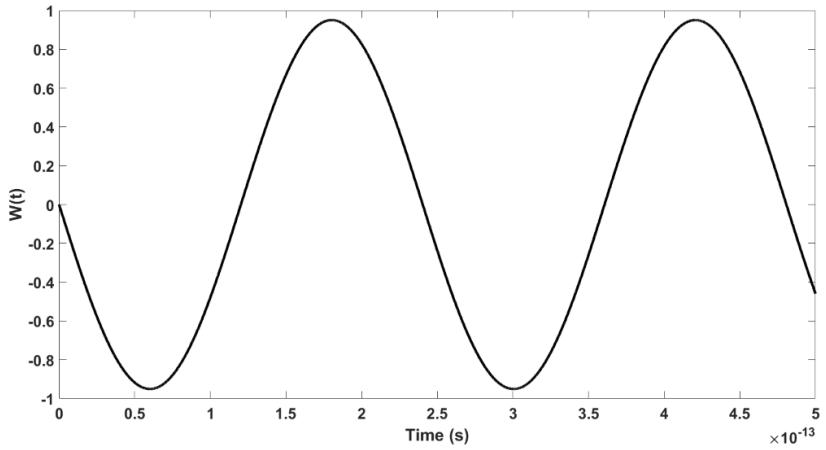

Figure 4: The population inversion $W(t)$ by setting $\alpha = 1$, $\beta = 1$, and $\gamma = 0.4$

Figure 5 shows $W(t)$ when $\beta = 0.8$ and $\gamma = 1$. When β is less than 1, the frequency of $W(t)$ is significantly reduced when compared with $W(t)$ in Figure 1. The same effect is observed in Figures 6 and 7 by setting $\gamma = 1$ and adjusting β to 0.625 and 0.4, respectively. Note that adjusting γ results in fewer population inversion changes than adjusting β.

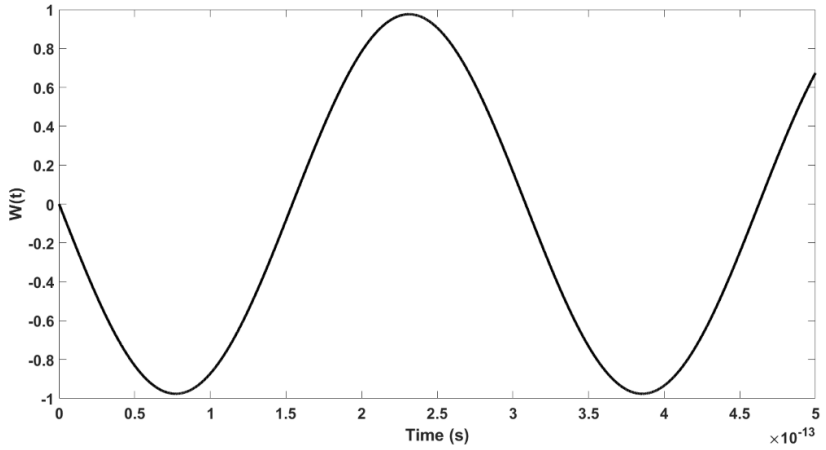

Figure 5: The population inversion $W(t)$ by setting $\alpha = 1$, $\beta = 0.8$, and $\gamma = 1$

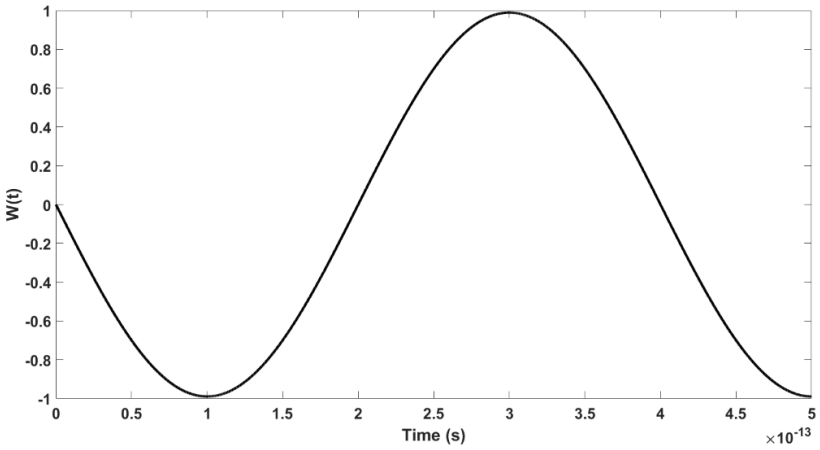

Figure 6: The population inversion $W(t)$ by setting $\alpha = 1$, $\beta = 0.625$, and $\gamma = 1$

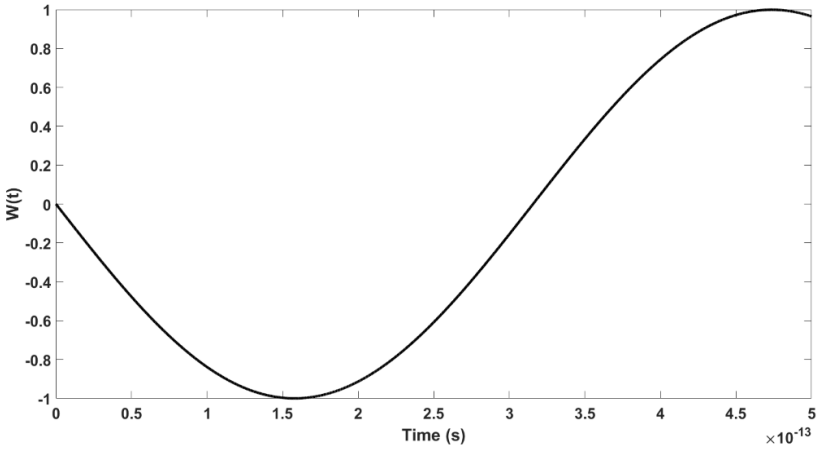

Figure 7: The population inversion $W(t)$ by setting $\alpha = 1$, $\beta = 0.4$, and $\gamma = 1$

4.2 The Population Inversion $W(t)$ from The Conformable Maxwell–Schrodinger Equations by Adjusting α

We defined the fractional conformable function $\varphi(x, \alpha)$ as the Khalil's definition, which is $\varphi(x, \alpha) = x^{1-\alpha}$ [18], and we set both β and γ to 1 then adjusted α. The resulting $W(t)$ from setting $\alpha = 0.999$, $\beta = 1$, and $\gamma = 1$ is shown in Figure 8. We can see that when α is less than 1, the smooth-

ness of $W(t)$ decreases, and the frequency of the population inversion $W(t)$ increases, suggesting that the time required to complete the waveform is reduced. Furthermore, the peak of the oscillation is reduced. These results are significantly different when compared with the case, described in Figure 1, of setting $\alpha = 1$. The same effect can be seen in Figures 9 and 10 by setting $\gamma = 1$, $\beta = 1$, and adjusting α from 0.995 to 0.990.

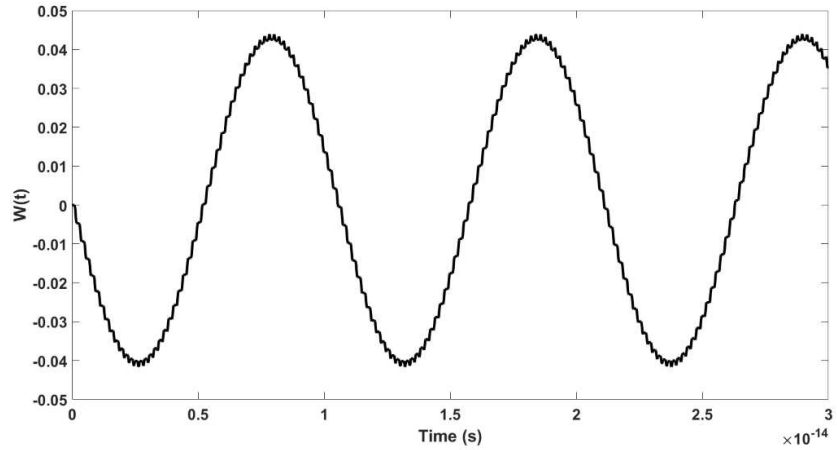

Figure 8: The population inversion $W(t)$ by setting $\alpha = 0.999$, $\beta = 1$, and $\gamma = 1$

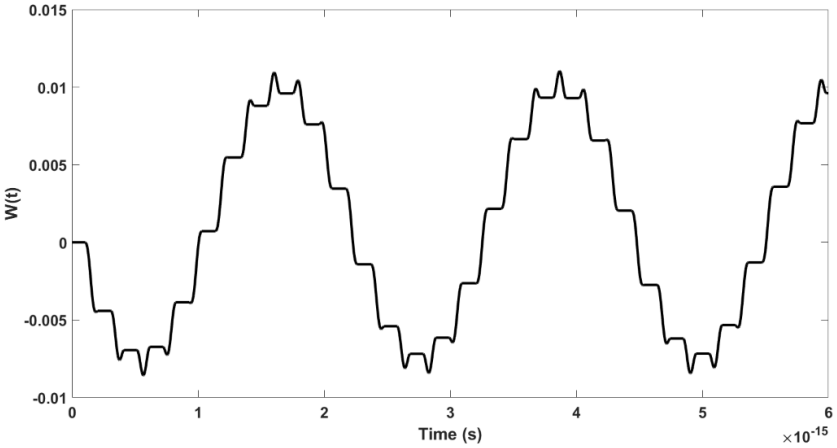

Figure 9: The population inversion $W(t)$ by setting $\alpha = 0.995$, $\beta = 1$, and $\gamma = 1$

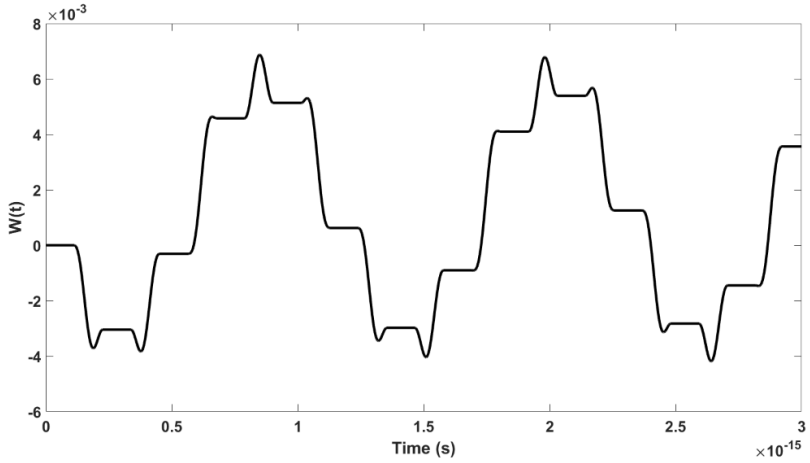

Figure 10: The population inversion $W(t)$ by setting $\alpha = 0.990$, $\beta = 1$, and $\gamma = 1$

Figures 11 and 12 show $W(t)$ when $\alpha = 0.999$, $\beta = 1$ and γ varies. The changes in $W(t)$ are difficult to see, and we will conclude that adjusting the γ shift has no significant effect on the population inversion. A similar effect can be seen in Figures 13 and 14 by setting $\alpha = 0.995$, $\beta = 1$, and adjusting γ.

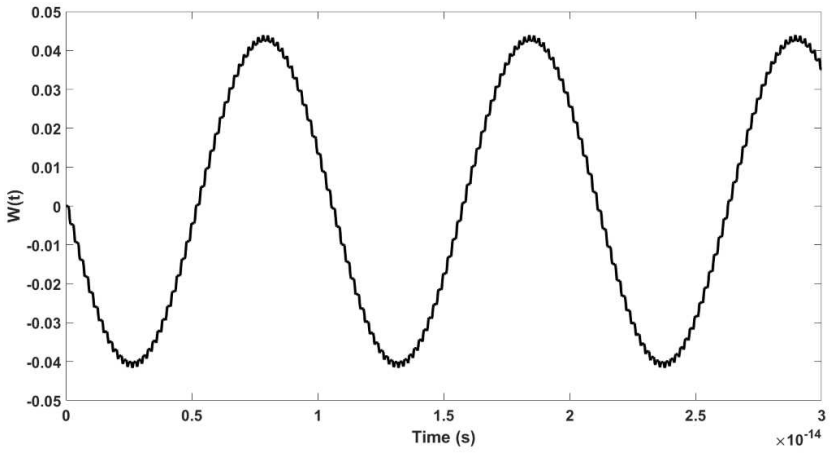

Figure 11: The population inversion $W(t)$ by setting $\alpha = 0.999$, $\beta = 1$, and $\gamma = 0.8$

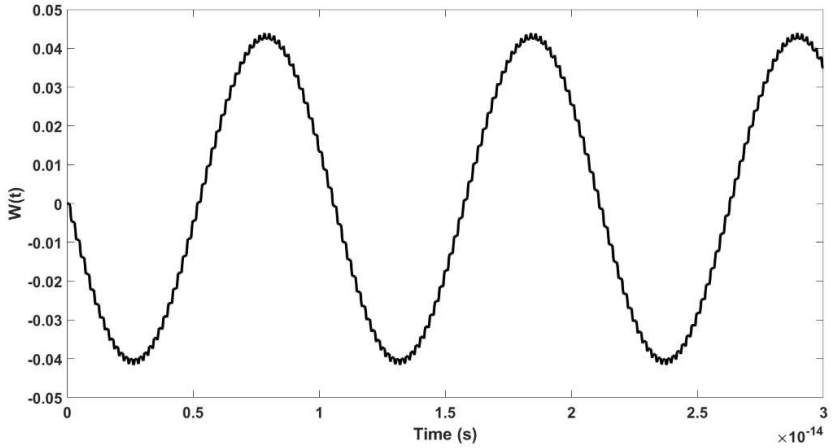

Figure 12: The population inversion $W(t)$ by setting $\alpha = 0.999$, $\beta = 1$, and $\gamma = 0.625$

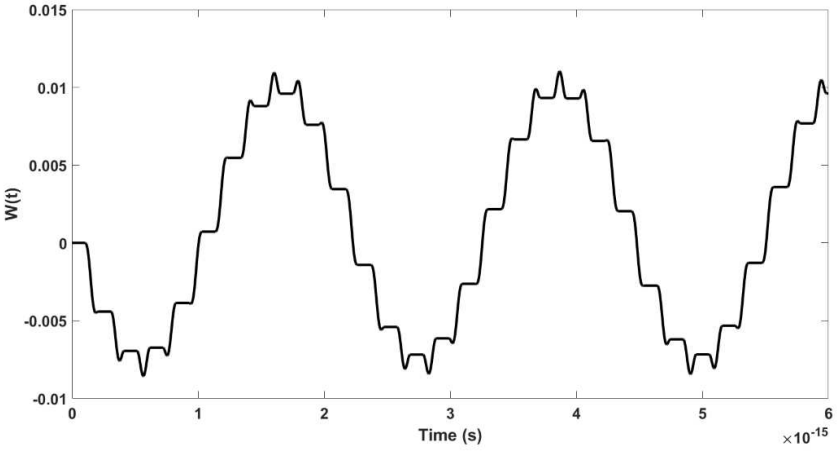

Figure 13: The population inversion $W(t)$ by setting $\alpha = 0.995$, $\beta = 1$, and $\gamma = 0.8$

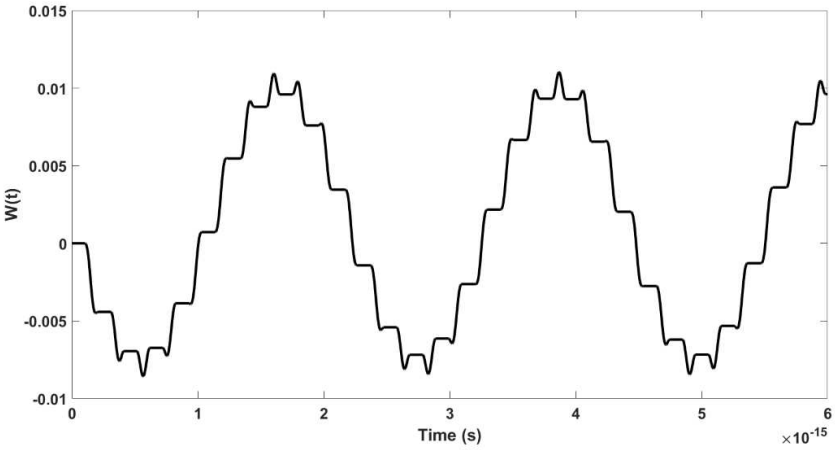

Figure 14: The population inversion $W(t)$ by setting $\alpha = 0.995$, $\beta = 1$, and $\gamma = 0.625$

Figures 15 and 16 show $W(t)$ by setting $\alpha = 0.999$, $\gamma = 1$, and adjusting β. When β is less than 1, the amplitude of $W(t)$ are lower. The same effect can be seen in Figures 17 and 18 by setting $\alpha = 0.995$, $\gamma = 1$, and adjusting β. Importantly, adjusting γ results in fewer changes to the population inversion than adjusting β.

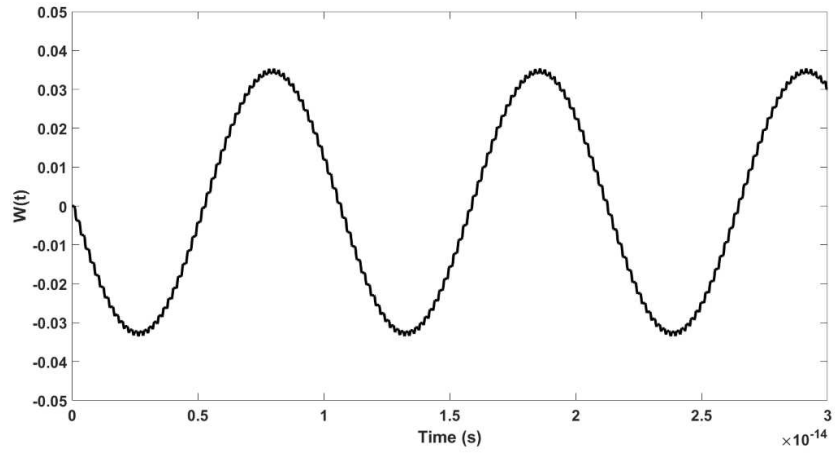

Figure 15: The population inversion $W(t)$ by setting $\alpha = 0.999$, $\beta = 0.8$, and $\gamma = 1$

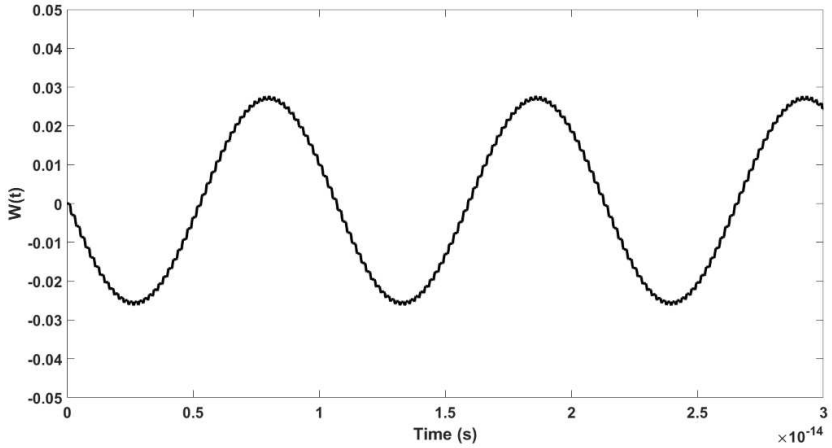

Figure 16: The population inversion $W(t)$ by setting $\alpha = 0.999$, $\beta = 0.625$, and $\gamma = 1$

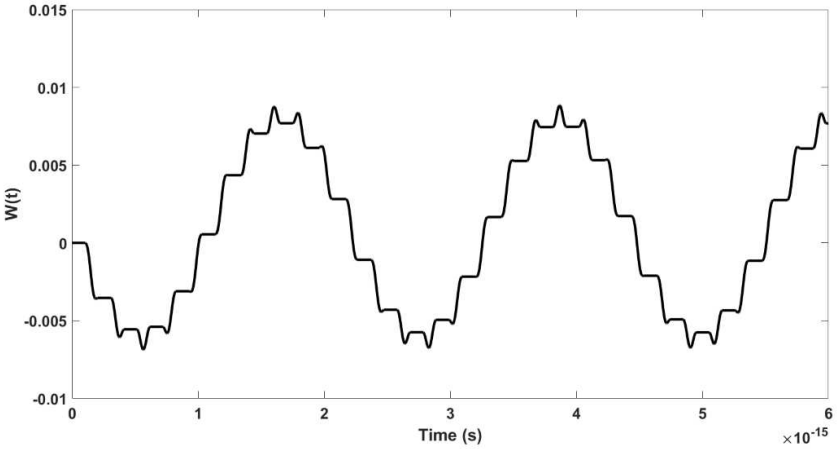

Figure 17: The population inversion $W(t)$ by setting $\alpha = 0.995$, $\beta = 0.8$, and $\gamma = 1$

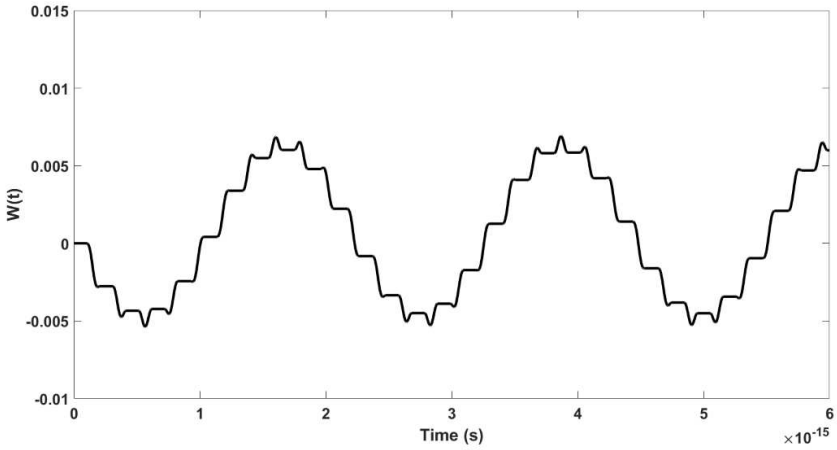

Figure 18: The population inversion $W(t)$ by setting $\alpha = 0.995$, $\beta = 0.625$, and $\gamma = 1$

5 Conclusion

Here, we have presented a fractional FDTD method to solve the conformable Maxwell-Schrodinger equations. We found the numerical solution and obtained it in the population inversion, which was divided into two cases.

In the first case, when we set $\alpha = 1$, the conformable Maxwell-Schrodinger equations turned into the classical model. The population inversion looked wavelike, oscillating between its ground state and its excited state. When adjusting γ to less than 1, the frequency of the population inversion increased, which resulted in β becoming less than 1. Furthermore, when γ was adjusted, the population inversion changed very little in comparison with β adjustments. This was because the time-step was small in comparison to the size-step.

In the second case, we adjusted α to less than 1. This caused the frequency of the population inversion to increase, but there was a noticeable loss of smoothness and oscillation. Adjusting γ had little effect when compared with changing β, similarly to the first case. When adjusting β to less than 1, the oscillations of the population inversion were lower.

Acknowledgment. This research was partially supported by a research grant from the Department of Mathematics, King Mongkut's University of Technology Thonburi (KMUTT).

References

[1] J.C. Maxwell, A Dynamical Theory of the Electromagnetic Field, Phil. Trans. R. Soc. London, **155,** (1864), 459–512.

[2] D.L. Sengupta, T.K. Sarkar, A Dynamical Maxwell, Hertz, the Maxwellians, and the Early History of Electromagnetic Waves, IEEE Antennas and Propagation Magazine, **45,** no. 2, (2003), 13–19.

[3] K.B. Oldham, J. Spanier, The Fractional Calculus Theory and Applications of Differentiation and Integration to Arbitrary Order, Academic Press, London, 1974.

[4] I. Podlubny, Fractional Differential Equations: An Introduction to Fractional Derivatives, Fractional Differential Equations, to Methods of their Solution and Some of Their Applications, Academic Press, California, 1999.

[5] A.M. Mathai, H.J. Haubold, An Introduction to Fractional Calculus, Nova Science Publishers, New York, 2017.

[6] V.E. Tarasov, Fractional Vector Calculus and Fractional Maxwell's Equations, Annals of Physics, **323,** no. 11, (2008), 2756–2778.

[7] D. Zhao, M. Luo, General conformable fractional derivative and its physical interpretation, Calcolo, **54,** (2017), 903–917.

[8] D. Zhao, X. Pan, M. Luo, A new framework for multivariate general conformable fractional calculus and potential applications, Physica A, **510,** (2018), 271–280.

[9] Y.P. Chen, W.E.X. Sha, L. Jiang, M. Meng, Y.M. Wu, W.C. Chew, A unified hamiltonian solution to maxwell–schrodinger equations for modeling electromagnetic field–particle interaction, Computer Physics Communications, **215,** (2017), 63–70.

[10] M. Oxborrow, J.D. Breeze, N.M. Alford, Room-temperature solid-state maser, Nature, **488,** (2012), 353–356.

[11] B. Ellis, M.A. Mayer, G. Shambat, T. Sarmiento, J. Harris, E.E. Haller, J. Vuckovic, Ultralow-threshold electrically pumped quantum-dot photonic-crystal nanocavity laser, Nature Photonics, **5,** (2011), 297–300.

[12] L.C. Andreani, G. Panzarini, J.M. Gerard, Strong-coupling regime for quantum boxes in pillar microcavities: Theory, Physical Review B, **60,** (1999), 13276–13279.

[13] T. Hummer, F.J. Garcia-Vidal, L. Martin-Moreno, D. Zueco, Weak and strong coupling regimes in plasmonic QED, Physical Review B, **87,** (2013), 115419.

[14] T. Rylander, P. Ingelstrom, A. Bondeson, Computational Electromagnetics, Springer, New York, 2013.

[15] K. Yee, Numerical solution of initial boundary value problems involving maxwell's equations in isotropic media, IEEE Transactions on Antennas and Propagation, **14,** no. 3, (1966), 302–307.

[16] A. Atangana, Fractional discretization: The African's tortoise walk, Chaos, Solitons and Fractals, **130,** (2020), 1093991–1-109399-24.

[17] C. Gerry, P. Knight, Introductory Quantum Optics, Cambridge University Press, New York, 2005.

[18] R. Khalil, M. Al Horani, A. Yousef, M. Sababheh, A new definition of fractional derivative, Journal of Computational and Applied Mathematics, **264,** (2014), 65–70.